Biochimica et Biophysica Acta 1808 (2011) 589–596

Contents lists available at ScienceDirect

Biochimica et Biophysica Acta

journal homepage: www.elsevier.com/locate/bbamem

Sodium–calcium exchanger and lipid rafts in pig coronary artery smooth muscle

Iwona Kuszczak [b], Sue E. Samson [a], Jyoti Pande [a], Dana Q. Shen [a], Ashok K. Grover [a,b,*]

[a] Department of Medicine, McMaster University, Hamilton, Ontario, Canada
[b] Department of Biology, McMaster University, Hamilton, Ontario, Canada

ARTICLE INFO

Article history:
Received 4 July 2010
Received in revised form 11 November 2010
Accepted 23 November 2010
Available online 3 December 2010

Keywords:
NCX1
SERCA2
Caveolin
Fluorescence microscopy
Lipid raft

ABSTRACT

Pig coronary artery smooth muscle expresses, among many other proteins, Na^+–Ca^{2+}-exchanger NCX1 and sarcoplasmic reticulum Ca^{2+} pump SERCA2. NCX1 has been proposed to play a role in refilling the sarcoplasmic reticulum Ca^{2+} pool suggesting a functional linkage between the two proteins. We hypothesized that this functional linkage may require close apposition of SERCA2 and NCX1 involving regions of plasma membrane like lipid rafts. Lipid rafts are specialized membrane microdomains that appear as platforms to co-localize proteins. To determine the distribution of NCX1, SERCA2 and lipid rafts, we isolated microsomes from the smooth muscle tissue, treated them with non-ionic detergent and obtained fractions of different densities by sucrose density gradient centrifugal flotation. We examined the distribution of NCX1; SERCA2; non-lipid raft plasma membrane marker transferrin receptor protein; lipid raft markers caveolin-1, flotillin-2, prion protein, GM1-gangliosides and cholesterol; and cytoskeletal markers clathrin, actin and myosin. Distribution of markers identified two subsets of lipid rafts that differ in their components. One subset is rich in caveolin-1 and flotillin-2 and the other in GM1-gangliosides, prion protein and cholesterol. NCX1 distribution correlated strongly with SERCA2, caveolin-1 and flotillin-2, less strongly with the other membrane markers and negatively with the cytoskeletal markers. These experiments were repeated with a non-detergent method of treating microsomes with sonication at high pH and similar results were obtained. These observations are consistent with the observed functional linkage between NCX1 and SERCA2 and suggest a role for NCX1 in supplying Ca^{2+} for refilling the sarcoplasmic reticulum.

1. Introduction

Coronary arteries supply blood to the heart. Since drastic changes in the blood flow may lead to cardiac disorders, the coronary blood flow is tightly regulated [1–4]. Control of cytosolic Ca^{2+} (Ca^{2+}i) is pivotal to pulsatile action of the coronary artery smooth muscle. Ca^{2+}i increases during muscle contraction, following which it decreases to resting levels during muscle relaxation. Three major transport systems contribute to this decrease in Ca^{2+}i: Na^+–Ca^{2+}- exchanger (NCX), plasma membrane (PM) Ca^{2+} pump (PMCA) and sarcoplasmic reticulum (SR) Ca^{2+} pump (SERCA) [4–15]. The pig coronary artery smooth muscle expresses proteins NCX1, SERCA2 and PMCA1 and 4 [16]. Depending on the electrochemical gradients, NCX can move Ca^{2+} into or out of the cell. We have shown that NCX mediated Ca^{2+} entry in smooth muscle cells cultured from pig coronary artery is diminished in the presence of the SERCA inhibitor thapsigargin [17]. However, cells preloaded with a Ca^{2+} chelator show an increase in NCX mediated Ca^{2+} entry without any inhibition by thapsigargin (Supplemental Data Fig. S1). These results suggest a functional linkage between NCX1 and SERCA2 in the smooth muscle cells. Similarly, other studies showing the role of NCX in refilling Ca^{2+} pool of SR in conjunction with SERCA also suggest a functional linkage between the two proteins [5,6,18–23]. Several models have been proposed to explain this linkage. One model based on Ca^{2+}i measurements in resting smooth muscle of rabbit vena cava shows the rapid cycling of Ca^{2+} between the SR and the extracellular space by SERCA and NCX. The close apposition of the PM and the SR allows the preferential release of Ca^{2+} from the SR towards NCX. When NCX is blocked by removing both the external Na^+ and Ca^{2+}, Ca^{2+} released from the SR is sequestered back by SERCA. Only when both NCX and SERCA are blocked is the Ca^{2+} released from the SR expelled to the extracellular space by PMCA [19,24]. In another model, the spatial distribution of the PM containing NCX is shown to be closely apposed to the SR membrane containing SERCA [20]. This suggestion is based on co-distribution of NCX and the Na^+/K^+ pump in the PM with calsequestrin rich superficial SR [9,18,19,23–25]. Immunofluorescence microscopy with cells cultured from pig coronary artery smooth muscle show NCX1 in proximity to SERCA2 [26].

In some instances, a direct protein–protein interaction has been proposed between different ion transporters. In others, it is suggested that lipid rafts act as the intermediaries allowing the assembly and

Abbreviations: Ca^{2+}i, cytosolic Ca^{2+}; EGTA, ethyleneglycol bis (2-aminoethyl ether)-N,N,N′,N′-tetraacetic acid; NCX, Na^+–Ca^{2+}-exchanger; PBS, phosphate buffered saline; PM, plasma membrane; PMCA, PM Ca^{2+} pump; SR, sarcoplasmic reticulum; SERCA, SR Ca^{2+} pump

* Corresponding author. Department of Medicine, McMaster University, Hamilton, Ontario, Canada L8N3Z5. Tel.: +1 905 525 9140x22238; fax: +1 905 522 3114.
E-mail address: groverak@mcmaster.ca (A.K. Grover).

0005-2736/$ – see front matter © 2010 Elsevier B.V. All rights reserved.
doi:10.1016/j.bbamem.2010.11.029

interaction of various proteins. Lipid rafts are cholesterol and sphingolipid rich domains in the PM [27,28]. Lipid rafts have been shown to be involved in the interactions between the SR resident protein STIM1 and the PM protein Orai1 [29]. The lipid rafts may be planar or invaginated [27,28]. The invaginated domains are termed caveolae and are rich in the protein caveolin. Caveolin is encoded by different genes of which caveolin-1 is expressed in the pig coronary artery smooth muscle [30–32]. Several studies based on immunofluorescence and electron microscopy link the SR with caveolae in smooth muscle [19,21,33,34].

The lipid rafts are not solubilized in low concentrations of non-ionic detergents. This property can be exploited to fractionate membranes to separate low density, detergent resistant membrane fractions on density gradients and examine the protein distributions [27,30–32]. Membranes can also be fractionated by a non-detergent based method that involves treatment with high pH and sonication followed by separation on density gradients [31,35,36]. The present work uses both methods to determine if membrane fractions containing proteins NCX1 and SERCA2 co-migrate in density flotation experiments.

2. Methods

2.1. Isolation of microsomes

Smooth muscle from coronary arteries of pig hearts (Maple Leaf Foods, Burlington) was dissected and used for isolating microsomes at 4 °C with minor modifications of a previously described method [37]. Briefly, the isolated smooth muscle tissue was homogenized in a homogenization solution containing 8% sucrose (wt./wt.) and the following in millimolar: 2 dithiothreitol, 1 phenylmethylsulfonyl-fluoride, 100 KCl and 0.05 ethyleneglycol bis (2-aminoethyl ether)-N, N,N′,N′-tetraacetic acid (EGTA). The samples were centrifuged at 10,000*g* for 10 min and the supernatant was saved. The pellet from this step was homogenized and centrifuged again to obtain the supernatant. The two supernatants were pooled and filtered through cheesecloth, KCl was added to a final concentration of 700 mM and the sample stirred for 15 min at 4 °C. The sample was then centrifuged at 388,000*g* for 30 min at 4 °C and the pellet (microsomes) was suspended in a solubilization buffer containing 8% sucrose (wt./wt.) and the following in millimolar: 15 imidazole-HCl (pH 7.0), 150 NaCl, 0.05 EGTA and 0.25 dithiothreitol. The suspension was centrifuged again at 388,000*g* for 20 min, and the resulting pellet was termed microsomes and suspended in the same buffer.

2.2. Determination of detergent concentration to solubilize protein

A highly concentrated microsomal suspension (12 mg protein/ml) was used in fractionation experiments to observe the distribution of various markers in each sucrose density gradient fraction. To determine the optimal detergent concentration, the microsomal suspension (12 mg/ml) was treated with specified concentrations of Triton X-100 and allowed to mix by rotation for 30 min at 4 °C. The samples were then centrifuged in a Beckman Airfuge at 200,000*g* for 20 min. The supernatant (S) and the pellets (P) were used for the analysis of distribution of various markers by Western blot. The amount of the solubilized protein in the supernatant was determined as percent of the total protein in the supernatant and pellet $(S/(S+P)\times 100)$ as determined from the band intensities in Western blot.

2.3. Flotation of detergent treated microsomes on density gradients

The microsomal suspension (12 mg protein/ml) was treated with Triton X-100 (final 0.15%) by rotation for 30 min at 4 °C. Then, 600 µl of 60% sucrose was added to 300 µl of the detergent treated sample to obtain a uniform suspension. This suspension was pipetted into the bottom of a swinging bucket rotor tube and a gradient was prepared by layering successive decreasing sucrose density solutions (37%, 34%, 29%, 25%, 20% and 15%) and the tubes were centrifuged at 278,000*g* for 20 h at 4 °C. Fractions were collected starting from the top, aliquoted and saved at −80 °C for analysis.

A similar experiment was also conducted by sonication. The microsomal pellet was suspended in 400 µl of 500 mM sodium carbonate (pH 11). The microsomes were then subjected to three cycles of sonication (Fisher sonicator) on ice at 80% power in 20 s bursts and one cycle of 60 s. A buffer (50 µl of 250 mM 2-(N-morpholino) ethanesulfonic acid, 1.5 M NaCl, pH 6.5) and then 800 µl of 60% sucrose were added. The suspension was subjected to flotation by sucrose density gradient centrifugation as described above for the detergent treated microsomes. Total protein concentration of each sucrose density gradient fraction was determined using Bradford reagent (BioRad, Mississauga, ON).

2.4. Western blots and biochemical determinations

Sources and selectivity of the various antibodies used are shown in Table 1. Western blots were treated with the primary antibodies and horseradish peroxidase conjugated anti-mouse IgG or anti-rabbit IgG. The peroxidase activity was visualized with a femto-kit (Pierce Chemical Company, Rockford) and a LAS3000 mini Luminiscent Image Analyzer (Fujifilm Life Science, Stamford, CT). Antibodies used in the experiments were tested in the initial Western blots with microsomes to identify the optimal protein concentration for detection and the location of correct molecular weight bands (Fig. S2). GM1-gangliosides were detected in dot blots using horseradish peroxidase conjugated cholera toxin B subunit. Cholesterol determination was carried out fluorometrically using an Amplex Red Kit (A12216) following instructions of the manufacturer (Invitrogen, Burlington, Canada).

Table 1
Sources of antibodies.

Antibody	Selectivity	Source
IID8	Anti-SERCA2	Affinity Bioreagents, Golden, USA
4G5	Anti-SERCA2	Gift from Dr. L.R. JONES, Indianapolis,USA
5F10	Anti-PMCA (PMCA1–4)	Affinity Bioreagents, Golden, USA
JA9	Anti-PMCA4	Sigma, St. Louis, Missouri, USA
R3F1	Anti-NCX1	Swant Swiss Antibodies, Bellinzona
1A4	Anti-smooth muscle actin	Sigma, St. Louis, Missouri, USA
6H4	Anti-prion protein	Prionics AG, Switzerland
Anti-MHC2	Anti-smooth muscle myosin heavy chain 2	Abcam Inc., Cambridge, MA, USA
23	Anti-clathrin heavy chain	BD Biosciences, Mississauga, Canada
2297	Anti-caveolin-1	BD Biosciences, Mississauga, Canada
29/flotillin-2	Anti-flotillin-2/ESA	BD Biosciences, Mississauga, Canada
HRP–anti-mouse IgG	HRP-conjugated anti-mouse IgG	Sigma, St. Louis, Missouri, USA
HRP–anti-rabbit IgG	HRP-conjugated anti-rabbit IgG	Sigma, St. Louis, Missouri, USA
HRP–cholera toxin subunit B	Detects GM gangliosides	Sigma, St. Louis, Missouri, USA
Anti-mouse-488	Alexa Fluor 488 goat anti-mouse IgG	Invitrogen, Burlington, Canada
Anti-mouse-568	Alexa Fluor 568 goat anti-mouse IgG	Invitrogen, Burlington, Canada
Anti-rabbit-568	Alexa Fluor 568 goat anti-rabbit IgG	Invitrogen, Burlington, Canada

2.5. Statistical analysis

Intensities in Western blots were determined using Multi Gauge v3.0 (Fujifilm Life Science, Stamford, USA). Correlations between relative intensities of proteins in Western blots were analyzed using GraphPad InStat (San Diego, USA). *P* values <0.05 were considered to be significant.

3. Results

In literature, two main methods have been used to isolate the lipid raft membrane fraction in sucrose density gradients: non-ionic detergents and high pH with ultrasonication [30–32,35,36,38]. For comparison, both methods were used in this study.

3.1. Determination of detergent concentration to solubilize protein

In one set of experiments, microsomes suspended in buffer containing 8% sucrose were treated with different concentrations of Triton X-100 and centrifuged to obtain a supernatant as the detergent soluble fraction and a pellet as the detergent resistant fraction. The effect of increasing concentrations of Triton X-100 on the solubilization of a concentrated microsomal suspension (12 mg protein/ml) as determined by Western blot of various proteins is shown in Fig. 1. At all concentrations of Triton X-100 tested, the lipid raft markers caveolin-1 and flotillin-2 were found mainly in the detergent resistant fraction. The amount of the non-lipid raft plasma membrane marker transferrin receptor protein in the soluble fraction increased with the increasing detergent concentrations. Similarly, the amounts of solubilized NCX1 and SERCA2 in the supernatant increased with the increasing Triton X-100 concentrations, with their value in supernatant as percent of total showing an excellent correlation (Pearson correlation coefficient = 0.9732). Approximately half of the total NCX1 protein was solubilized at 0.15% (1.5 mg Triton X-100/ml) detergent concentration. This detergent:protein ratio was used in the next experiment in which microsomes at a concentration of 12 mg protein/ml were treated with 0.15% Triton X-100 and fractionated by membrane flotation on a sucrose density gradient.

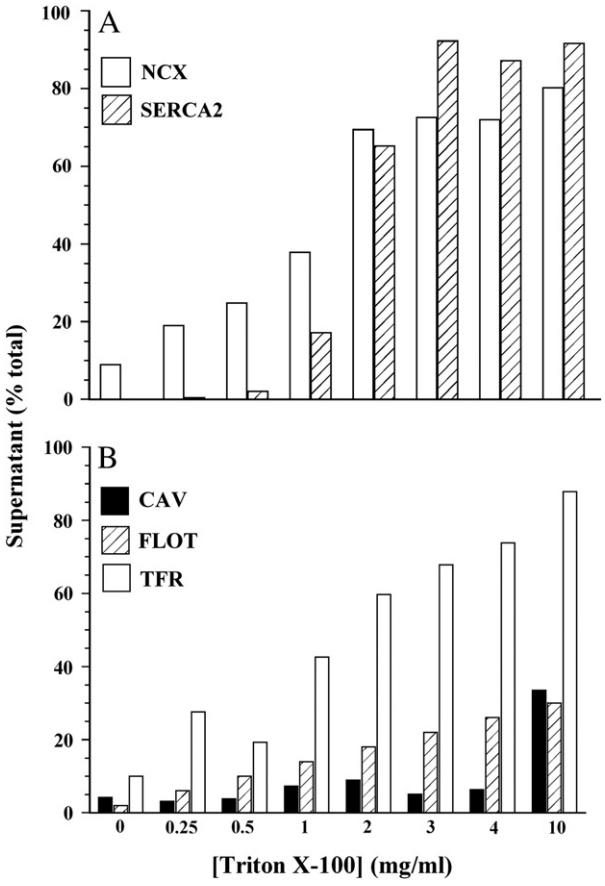

Fig. 1. Effect of different concentrations of Triton X-100 on solubilization of 12 mg/ml of microsomal proteins. The amount of each protein was analyzed in Western blots. Percent of the amount that appeared in the supernatant (solubilized) at each detergent concentration is shown. A. NCX1 and SERCA2. B. CAV (caveolin-1), FLOT (flotillin-2) and TFR (transferrin receptor protein).

3.2. Flotation of detergent treated microsomes

The detergent (0.15% Triton X-100) treated microsomes (12 mg protein/ml) were suspended in a high sucrose concentration and centrifuged in a sucrose density gradient. Upon centrifugation, the detergent resistant fraction of microsomes floats to the low density regions of the sucrose gradient. Based on the protein contents, determined using Bradford reagent, in the density gradient fractions, most of the microsomal protein was detergent soluble as it remained in the high density fraction (Fig. 2B). In contrast, the low density fractions were most enriched in cholesterol. The distribution of the following markers in the density gradient was examined in Western blots: NCX1, SERCA2, lipid raft markers (flotillin-2, prion protein, GM1 gangliosides and caveolin), non-lipid raft marker (transferrin receptor protein) and cytoskeletal proteins (clathrin, actin and myosin) (Fig. 2A). The amount of marker in each density gradient fraction was obtained by quantification of Western blots by densitometric analysis is expressed as percent of the fraction with its highest amount (Fig. 2C–G).

The lipid raft markers GM1-gangliosides, prion protein and cholesterol were enriched in the lowest density gradient fraction (sucrose 20%) and showed a monotonic decrease in their abundance in fractions with increasing sucrose density (Fig. 2A and E). The decrease was slightly less steep for cholesterol than the other two markers (Fig. 2E). In contrast, the amount of flotillin-2 and caveolin-1 increased in fractions of increasing densities and peaked at sucrose density ranges 24%–27% and 27%–33%, respectively. They showed a decrease in abundance in the fractions with higher sucrose densities (Fig. 2D). These distributions of lipid raft markers were confirmed in experiments using five microsomal preparations. Thus, the distribution of various lipid raft markers in density gradients differs from each other (Fig. S3) and identifies two subsets of lipid rafts: those that are rich in caveolin-1 and flotillin-2 and others that have GM1-gangliosides, prion protein and cholesterol as their components.

NCX1 co-migrated with SERCA2 (Fig. 2C) and showed a distribution pattern more similar to that observed for caveolin-1 and flotillin-2 than for GM1-gangliosides, prion protein, cholesterol and transferrin receptor protein in various density gradient fractions (Fig. 2D, E and G). It did not show association with cytoskeletal markers that were enriched in the high density gradient fraction (sucrose 44%) (Fig. 2F). Pearson's coefficients for correlation of NCX1 distribution with that of lipid and non-lipid raft markers in sucrose gradient were determined (Fig. 3). NCX1 distribution showed positive and significant correlation with SERCA2. It showed a higher correlation of distribution with caveolin-1 and flotillin-2 in density gradient fractions as compared to other lipid raft markers (cholesterol, GM1-gangliosides and prion protein). NCX1 did not show significant correlation with the non-lipid raft marker transferrin receptor protein and showed negative correlation with the cytoskeletal markers clathrin, actin and myosin.

In another experiment which was repeated twice, the microsomes were treated with a much higher Triton X-100 concentration (1%) and then subjected to flotation by centrifugation in a sucrose gradient. The correlation between NCX1 and SERCA2 distribution in the density gradient in the two experiments were 0.699 and 0.79 (data not shown). Thus, the strength of correlation of migration of NCX1 and SERCA2 in

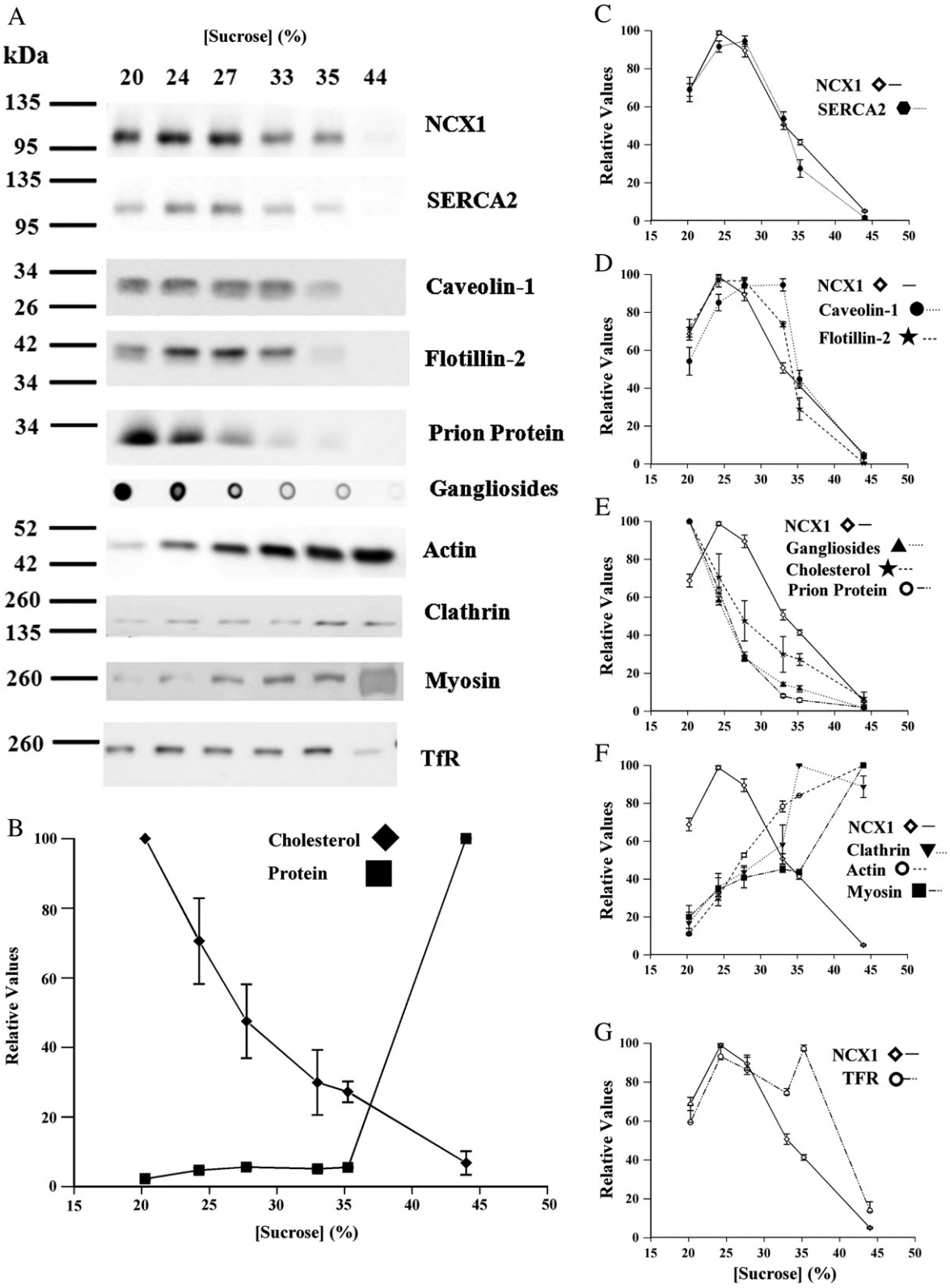

Fig. 2. Immunoblot analysis of marker distribution of detergent treated microsomes upon centrifugal flotation. A. Immunoblots. For Western blots, the amounts of protein loaded in microgram per well were 2 for NCX1, clathrin, myosin and transferrin receptor (TfR); 1 for SERCA2 and caveolin-1; 0.5 for flotillin-2 and prion protein and 0.2 for actin. Only the main bands for each of the proteins are shown with molecular weights in kilodalton on the left. Dot blots with 0.2 μg protein/spot were used for GM1-ganglioside detection. B. Relative values of total protein and cholesterol (per milligram protein) in various sucrose density gradient fractions. The density gradient fraction with the highest total protein or cholesterol per milligram protein was taken as 100% and their amount in other fractions are expressed relative to it. C–G. Graphs of relative enrichment of various markers in sucrose density gradient fractions as determined by Western blot. C. NCX1 and SERCA2. D. NCX1, caveolin-1 and flotillin-2. E. NCX1, GM1-gangliosides, cholesterol and prion protein. F. NCX1, clathrin, actin and myosin. G. NCX1 and transferrin receptor protein. For each marker, the gradient fraction with highest band intensity in a Western blot is taken as 100% and the band intensities of all other fractions are expressed relative to it (% maximum intensity). The values are mean ± SEM of 3–5 measurements using one membrane preparation.

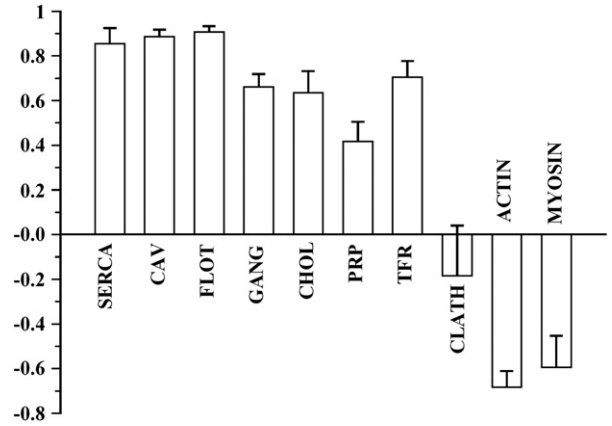

Fig. 3. Pearson's correlation between distributions of NCX1 and various markers in sucrose density gradient experiments using detergent. Mean ± SEM of the values of Pearson's coefficients obtained in five membrane preparations are shown.

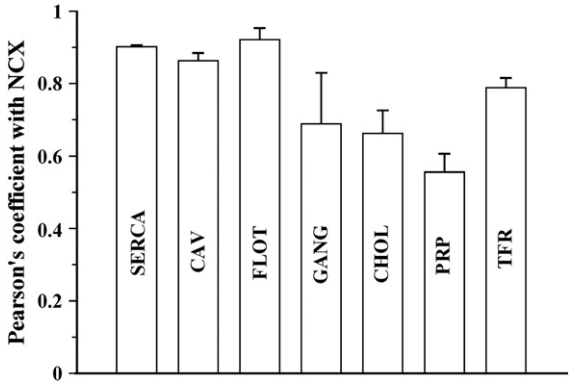

Fig. 5. Pearson's correlation between distributions of NCX1 and various markers in sucrose density gradient experiments using high pH and sonication. Mean ± SEM of the values of Pearson's coefficients [45] obtained in three membrane preparations are shown.

density gradient fractions observed at lower detergent concentration was retained even at six fold higher concentration of Triton X-100.

3.3. Flotation of sonicated microsomes on density gradients

Sonication of microsomes at high pH followed by flotation in a sucrose density gradient was also used to examine the distribution of various markers. As expected, most of the protein did not float to the lower density fractions of the sucrose gradient (Fig. S4). The distribution of various lipid raft and non-lipid raft markers in different density gradient fractions was similar to that observed with detergent treated microsomes (Fig. S4) NCX1 co-migrated with SERCA2 in density gradient fractions similar to that observed in detergent treated microsomes (Fig. 4). However, a key observation was that the SERCA2 protein bands were detected at molecular weights much larger than those observed with detergent treated microsomes (Fig. 4). Distribution of several markers was examined and values of the Pearson coefficients for correlation of NCX1 distribution with various markers were determined in this experiment in 2–4 microsomal preparations (Fig. 5). These results for co-distribution of NCX1 with SERCA and various lipid and non-lipid raft markers are similar to those observed with the detergent treated microsomes.

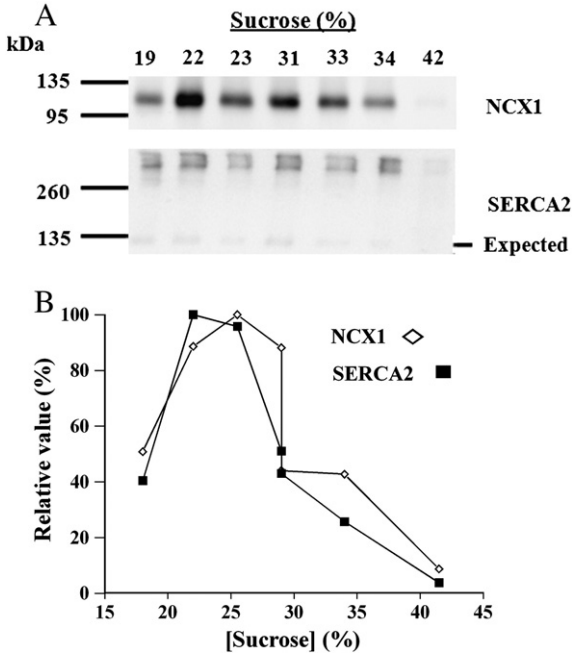

Fig. 4. Immunoblot analysis of NCX1 and SERCA2 distribution upon centrifugal flotation of microsomes treated with high pH-sonication. A. Western blots. Note that the molecular weight of SERCA2 without high pH-sonication treatment is marked 'expected.' B. Relative enrichment of NCX1 and SERCA2 in sucrose density gradient. The protocol and calculations were performed as for Fig. 2.

4. Discussion

Co-distribution of NCX1 and SERCA2 with lipid raft markers in the density gradient was observed both with the detergent and detergent free methods of preparing lipid rafts. However, the different lipid raft markers did not all partition together in the low density sucrose fractions. There appeared to be a close but not perfect association of NCX1 and SERCA2 with the lipid raft markers caveolin-1 and flotillin-2. This section focuses on the limitations of the methods used, comparison of the results with those in literature and their contribution to smooth muscle physiology.

Various methods have been used in literature to isolate detergent resistant lipid rafts with varied results [38–42]. Triton X-100 may selectively solubilize non-lipid raft domains of the membrane to allow for isolation of detergent resistant lipid rafts. However, detergents may contaminate the resulting lipid rafts, affect the buoyant density of rafts, cause individual rafts to coalesce or result in loss of raft resident proteins [42,43]. Therefore, the experiments were also repeated using a detergent free method using Na_2CO_3 to remove peripheral proteins followed by sonication to finely disrupt the membranes to study the distribution of various markers [35,43].

Alternative splicing of SERCA2 transcripts yields two proteins that differ in their C-terminal domains: SERCA2a and 2b. In pulmonary artery smooth muscle cells SERCA2a is present only in the perinuclear region while SERCA2b is in the superficial SR [44]. The commercially available anti-SERCA2 antibodies, including IID8, do not distinguish between the two variants. The present study to examine the distribution of SERCA2 using microsomes contains only the superficial SR and not nuclei [37]. However, since the nuclear envelope is a continuation of SR, the majority of microsomal markers are also found in the nuclear pellet [45]. We have shown previously that subcellular fractionation of smooth muscle from various sources including pig coronary artery to obtain an SR enriched fraction is accompanied by loss of yield. The activity of SERCA measured as oxalate dependent calcium uptake was used as a marker for SR enrichment in various fractions. Following tissue homogenization and initial centrifugation to remove nuclear pellet, less than 25% of total SERCA activity in postnuclear supernatant is associated with the microsomal pellet [37]. Centrifugation of microsomes on sucrose density gradient causes a further loss leading to an overall yield of only 18%. The Triton X-100

concentration chosen in our experiments would solubilize approximately 50% of total SERCA protein in microsomes (Fig. 1). The present study concerns only the SERCA2 and NCX1 present in the microsomes. This is consistent with our assumption that the SERCA2 that associates with NCX1 is mostly subsarcolemmal.

The migration of SERCA2 in a sucrose density gradient shows strong positive correlation with NCX1 and they distribute preferentially with flotillin-2 and caveolin-1 as compared to other lipid raft markers (Figs. 2C–E and 3). This co-distribution of SERCA2 and NCX1 with these lipid raft markers was observed at low (0.15% Triton X-100) and high (1% Triton X-100) detergent concentrations as well as by a detergent-free treatment of microsomes during membrane fractionation. This suggests that the observed co-distribution of proteins does not result due to any artifacts associated with the methods used; however, the exact nature of linkage between NCX1 and SERCA2 is not yet known. The formation of PM–SER junctions by close apposition of superficial SR to PM and caveolae has been reported in vascular smooth muscle [26,33,34,46,47]. Such junctions may allow ultrastructural arrangement of NCX1 and SERCA2 in nanospaces. Co-immunoprecipitation studies in neurons and astrocytes have shown linkage of NCX1 and SERCA2b in PM–SER junctions that involved cytoskeletal proteins ankyrin and spectrin [40]. Other studies have also suggested a role of yet unidentified anchoring molecules that are required to maintain PM–SER junctions or proteins which may also promote linkage of proteins in the two membranes. Stim–orai interaction is an example [29,48,49]. Lipid rafts mediate the clustering of STIM1 and Orai1 in the PM–SER junctions to facilitate their interaction to form a channel. In another study, both STIM1 and Orai1 are enriched in the same sucrose density gradient fractions as caveolin upon membrane fractionation following treatment with Na_2CO_3 and sonication [35,43,50]. The association of NCX1 and SERCA2 with a subset of lipid rafts suggests a role of these rafts in promoting their linkage. Co-distribution of SERCA2 with NCX1 may also result due to its interaction with other proteins of the PM lipid rafts or due to its targeting to the lipid raft-like domains in SR [51]. However, the nature of linkage in the pig coronary artery smooth muscle needs to be explored.

SERCA2 migrates as a high molecular weight protein instead of a 115 kDa band in Western blots following sonication of microsomes at high pH (Fig. 4). SERCA2 from pig coronary artery smooth muscle and other sources has been shown to be highly sensitive to changes in pH. The optimal Ca^{2+} transport activity of SERCA2 from pig coronary artery smooth muscle observed at pH 6.8 declines sharply with changes in pH [52]. The decline in activity is also accompanied by a decrease in the amount of 115 kDa Ca^{2+} dependent acylphosphate formed by SERCA during its reaction cycle. Similarly, inactivation of SERCA2b by other methods like treatment with reactive oxygen species involves the transition from its functionally active monomeric form to an oligomeric form [53]. Irrespective of migration of SERCA2 as a high molecular weight band in Western blots, it is important to note that its distribution pattern in various density gradient fractions is similar to that observed for the monomer with the detergent treated microsomes (Fig. 4). Thus, oligomerization does not appear to affect the SERCA2 distribution.

The importance of analyzing distribution patterns and linkages of proteins by more than one method is also emphasized by the discrepancy in the results of studies on co-localization of NCX1 and caveolin-3 in cardiac myocytes [54–56]. Therefore, we used two separate methods in the present study. The results from both the non-ionic detergent and sonication treatment of microsomes showed that there are subsets of lipid rafts: some rich in markers such as GM1-gangliosides, prion protein and possibly cholesterol and others rich in caveolin-1 and flotillin-2 (Figs. 3 and 5). The subsets rich in caveolin-1 would be those associated with caveolae. Studies have also shown localization of flotillin-2 in caveolae in other cell types [57–59]. These results are consistent with the heterogeneity of lipid rafts observed in the literature [27,39,60]. Lipid rafts have been described in coronary artery smooth muscle and other tissues as very small microdomains that may be less than 50 nm in size [27,61,62]. It is interesting to note that, in the present study with smooth muscle microsomes, NCX1 and SERCA2 co-migrated with caveolin-1 and flotillin-2 despite the heterogeneity and size of the lipid rafts (Figs. 2D and 3). The co-distribution of NCX1 and SERCA2 with a subset of lipid rafts is in agreement with studies that have shown the fraction of two proteins to be localized in PM–SER junctions, which in turn are closely associated with caveolae in smooth muscle cells. The present study used fresh tissues but similar co-localization of NCX1 and SERCA2 has also been observed in cells cultured from coronary artery smooth muscle by immunofluorescence microscopy which has a resolution of 200–300 nm [26].

The relationships between the transporters in the PM and the SR have been described by several models. They all lead to spatial units responsible for a vectorial control of free $[Ca^{2+}]i$ in defined nanospaces. It has also been suggested that the juxtaposition of the PM and the SR membranes may permit NCX1 to regulate SR Ca^{2+} stores and influence cellular Ca^{2+} signaling. Models for this type of function have been proposed for several cell types including cardiac myocytes and smooth muscle cells [5,21,36,38,40,63].

A superficial buffer barrier model was proposed initially to explain the results of Ca^{2+} flux studies [23]. This model has been extended to the idea of Ca^{2+} release units via PM–SER junctions, possibly also

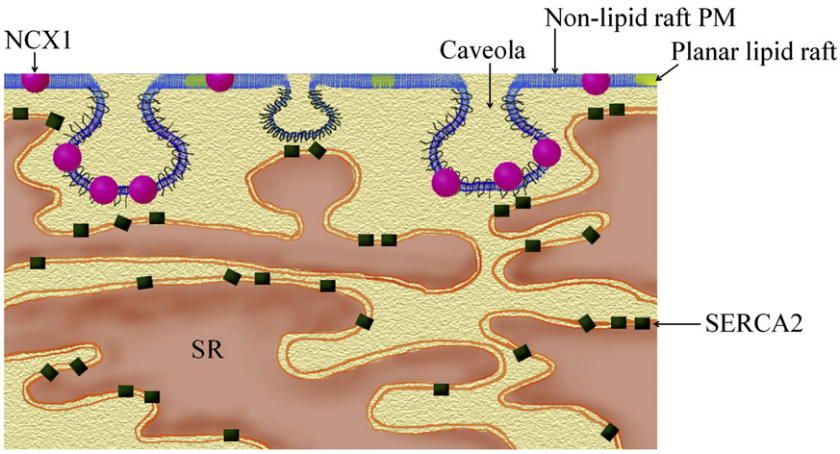

Fig. 6. A schematic model showing localization of NCX1, SERCA2 and caveolin-1 based on results from this work and from immunofluorescence microscopy. Caveolin-1 is shown as hairpin structures in the caveolar membrane. Note that the partial co-localization in this model reflects the less than total correlations observed in the distributions of NCX1 and SERCA2 with various markers.

involving NCX and nonspecific cation channels [18,19,21]. In support of this model, an association has been shown between distributions of calsequestrin, ryanodine receptors, and L-type Ca^{2+} channels [46]. Other groups have emphasized a functional role for caveolae as specialized Ca^{2+} handling domains [31,35]. In elegant studies using transmission electron microscopy, a model has been proposed for linking caveolae, SR and mitochondria [33,34]. In this model, caveolae, superficial SR and mitochondria are shown in close proximity of about 15 nm to create coherent cytoplasmic nanoscale subdomains. In this model, 80% of caveolae establish close contacts with SR. It is noted that the protein density in the organelles may be low and/or non-uniform and hence the organellar distances will often be smaller than those for the individual proteins in different organelles. Despite such differences, our current work and the work using transmission electron microscopy come to the same conclusion on co-localization of caveolae and SR. NCX1 was not examined in these studies. A model based on the present work and immunofluorescence overlap and proximity observed in the distribution of some of NCX1 and SERCA2 is proposed below. Fig. 6 is a schematic representation of our observations. PM contains non-lipid raft membrane with planar lipid raft domains and caveolae. NCX1 is proximal to caveolae but may also be present in other domains in PM. NCX1 in caveolae are in proximity with SERCA2 in the superficial SR. SERCA2 is also found in the deep SR that continues into the cytosol from the superficial SR. The ultrastructural arrangement of NCX1 and SERCA2 in proximity may allow NCX to supply Ca^{2+} for refilling the superficial SR. This model is also congruent with the role of caveolae in some Ca^{2+} signaling pathways. The full implications of this observation may need examination within the context of signal transduction pathways and tissue specificity.

Supplementary materials related to this article can be found online at doi: 10.1016/j.bbamem.2010.11.029.

Acknowledgements

This work was funded by a grant-in-aid from Heart and Stroke Foundation of Ontario (T6168, T6355).

References

[1] A.H. Lui, B.M. McManus, I. Laher, Endothelial and myogenic regulation of coronary artery tone in the mouse, Eur. J. Pharmacol. 410 (2000) 25–31.
[2] D. Merkus, D.J. Duncker, W.M. Chilian, Metabolic regulation of coronary vascular tone: role of endothelin-1, Am. J. Physiol. Heart Circ. Physiol. 283 (2002) H1915–H1921.
[3] F.T. Range, M. Schafers, T. Acil, K.P. Schafers, P. Kies, M. Paul, S. Hermann, B. Brisse, G. Breithardt, O. Schober, T. Wichter, Impaired myocardial perfusion and perfusion reserve associated with increased coronary resistance in persistent idiopathic atrial fibrillation, Eur. Heart J. 28 (2007) 2223–2230.
[4] J. Weirich, L. Dumont, G. Fleckenstein-Grun, Contribution of store-operated Ca2+ entry to pHo-dependent changes in vascular tone of porcine coronary smooth muscle, Cell Calcium 35 (2004) 9–20.
[5] M.P. Blaustein, W.J. Lederer, Sodium/calcium exchange: its physiological implications, Physiol. Rev. 79 (1999) 763–854.
[6] S. Bova, W.F. Goldman, X.J. Yauan, M.P. Blaustein, Influence of Na+ gradient on Ca2+ transients and contraction in vascular smooth muscle, Am. J. Physiol. 259 (1990) H409–H423.
[7] D.E. Clapham, Calcium signaling, Cell 131 (2007) 1047–1058.
[8] F. Di Leva, T. Domi, L. Fedrizzi, D. Lim, E. Carafoli, The plasma membrane Ca2+ ATPase of animal cells: structure, function and regulation, Arch. Biochem. Biophys. 476 (2008) 65–74.
[9] R. Floyd, S. Wray, Calcium transporters and signalling in smooth muscles, Cell Calcium 42 (2007) 467–476.
[10] A.K. Grover, I. Khan, Calcium pump isoforms: diversity, selectivity and plasticity. Review article, Cell Calcium 13 (1992) 9–17.
[11] J. Lytton, Na+/Ca2+ exchangers: three mammalian gene families control Ca2+ transport, Biochem. J. 406 (2007) 365–382.
[12] C.M. Misquitta, D.P. Mack, A.K. Grover, Sarco/endoplasmic reticulum Ca2+ (SERCA)-pumps: link to heart beats and calcium waves, Cell Calcium 25 (1999) 277–290.
[13] K.D. Philipson, D.A. Nicoll, Sodium–calcium exchange: a molecular perspective, Annu. Rev. Physiol. 62 (2000) 111–133.
[14] E.E. Strehler, A.J. Caride, A.G. Filoteo, Y. Xiong, J.T. Penniston, A. Enyedi, Plasma membrane Ca2+ ATPases as dynamic regulators of cellular calcium handling, Ann. N.Y. Acad. Sci. 1099 (2007) 226–236.
[15] F. Wuytack, Half a century of ion-transport ATPases: the P- and V-type ATPases, Pflugers Arch. 457 (2009) 569–571.
[16] M.M. Szewczyk, K.A. Davis, S.E. Samson, F. Simpson, P.K. Rangachari, A.K. Grover, Ca2+-pumps and Na2+–Ca2+-exchangers in coronary artery endothelium versus smooth muscle, J. Cell. Mol. Med. 11 (2007) 129–138.
[17] K.A. Davis, S.E. Samson, K.E. Hammel, L. Kiss, F. Fulop, A.K. Grover, Functional linkage of Na(+)–Ca(2+)-exchanger to sarco/endoplasmic reticulum Ca(2+) pump in coronary artery: comparison of smooth muscle and endothelial cells, J. Cell. Mol. Med. (2008).
[18] N. Fameli, C. van Breemen, K.H. Kuo, A quantitative model for linking Na+/Ca2+ exchanger to SERCA during refilling of the sarcoplasmic reticulum to sustain [Ca2+] oscillations in vascular smooth muscle, Cell Calcium 42 (2007) 565–575.
[19] C.H. Lee, D. Poburko, K.H. Kuo, C. Seow, C. van Breemen, Relationship between the sarcoplasmic reticulum and the plasma membrane, Novartis Found. Symp. 246 (2002) 26–41.
[20] E.D. Moore, E.F. Etter, K.D. Philipson, W.A. Carrington, K.E. Fogarty, L.M. Lifshitz, F.S. Fay, Coupling of the Na+/Ca2+ exchanger, Na+/K+ pump and sarcoplasmic reticulum in smooth muscle, Nature 365 (1993) 657–660.
[21] D. Poburko, K.H. Kuo, J. Dai, C.H. Lee, C. van Breemen, Organellar junctions promote targeted Ca2+ signaling in smooth muscle: why two membranes are better than one, Trends Pharmacol. Sci. 25 (2004) 8–15.
[22] M.K. Slodzinski, M.P. Blaustein, Physiological effects of Na+/Ca2+ exchanger knockdown by antisense oligodeoxynucleotides in arterial myocytes, Am. J. Physiol. 275 (1998) C251–C259.
[23] C. van Breemen, Q. Chen, I. Laher, Superficial buffer barrier function of smooth muscle sarcoplasmic reticulum, Trends Pharmacol. Sci. 16 (1995) 98–105.
[24] M.A. Nazer, C. van Breemen, Functional linkage of Na(+)–Ca2+ exchange and sarcoplasmic reticulum Ca2+ release mediates Ca2+ cycling in vascular smooth muscle, Cell Calcium 24 (1998) 275–283.
[25] M. Juhaszova, A. Ambesi, G.E. Lindenmayer, R.J. Bloch, M.P. Blaustein, Na(+)–Ca2+ exchanger in arteries: identification by immunoblotting and immunofluorescence microscopy, Am. J. Physiol. 266 (1994) C234–C242.
[26] I. Kuszczak, R. Kuner, S.E. Samson, A.K. Grover, Proximity of Na(+)–Ca (2+)-exchanger and sarco/endoplasmic reticulum Ca(2+) pump in pig coronary artery smooth muscle: fluorescence microscopy, Mol. Cell. Biochem. (2010).
[27] K. Jacobson, O.G. Mouritsen, R.G. Anderson, Lipid rafts: at a crossroad between cell biology and physics, Nat. Cell Biol. 9 (2007) 7–14.
[28] K. Simons, E. Ikonen, Functional rafts in cell membranes, Nature 387 (1997) 569–572.
[29] B. Pani, H.L. Ong, X. Liu, K. Rauser, I.S. Ambudkar, B.B. Singh, Lipid rafts determine clustering of STIM1 in endoplasmic reticulum–plasma membrane junctions and regulation of store-operated Ca2+ entry (SOCE), J. Biol. Chem. 283 (2008) 17333–17340.
[30] W.J. Cho, E.E. Daniel, Proteins of interstitial cells of Cajal and intestinal smooth muscle, colocalized with caveolin-1, Am. J. Physiol. Gastrointest. Liver Physiol. 288 (2005) G571–G585.
[31] E.E. Daniel, A. El Yazbi, W.J. Cho, Caveolae and calcium handling, a review and a hypothesis, J. Cell. Mol. Med. 10 (2006) 529–544.
[32] P.J. Darby, C.Y. Kwan, E.E. Daniel, Caveolae from canine airway smooth muscle contain the necessary components for a role in Ca(2+) handling, Am. J. Physiol. Lung Cell. Mol. Physiol. 279 (2000) L1226–L1235.
[33] M. Gherghiceanu, L.M. Popescu, Caveolar nanospaces in smooth muscle cells, J. Cell. Mol. Med. 10 (2006) 519–528.
[34] M. Gherghiceanu, L.M. Popescu, Electron microscope tomography: further demonstration of nanocontacts between caveolae and smooth muscle sarcoplasmic reticulum, J. Cell. Mol. Med. 11 (2007) 1416–1418.
[35] A.F. El Yazbi, W.J. Cho, R. Schulz, E.E. Daniel, Calcium extrusion by plasma membrane calcium pump is impaired in caveolin-1 knockout mouse small intestine, Eur. J. Pharmacol. 591 (2008) 80–87.
[36] W.I. Silva, H.M. Maldonado, M.P. Lisanti, J. Devellis, G. Chompre, N. Mayol, M. Ortiz, G. Velazquez, A. Maldonado, J. Montalvo, Identification of caveolae and caveolin in C6 glioma cells, Int. J. Dev. Neurosci. 17 (1999) 705–714.
[37] A.K. Grover, S.E. Samson, R.M. Lee, Subcellular fractionation of pig coronary artery smooth muscle, Biochim. Biophys. Acta 818 (1985) 191–199.
[38] M.R. Sepulveda, M. Berrocal-Carrillo, M. Gasset, A.M. Mata, The plasma membrane Ca2+-ATPase isoform 4 is localized in lipid rafts of cerebellum synaptic plasma membranes, J. Biol. Chem. 281 (2006) 447–453.
[39] S. George, M.D. Nelson, N. Dollahon, A. Bamezai, A novel approach to examining compositional heterogeneity of detergent-resistant lipid rafts, Immunol. Cell Biol. 84 (2006) 192–202.
[40] L. Lencesova, A. O'Neill, W.G. Resneck, R.J. Bloch, M.P. Blaustein, Plasma membrane–cytoskeleton–endoplasmic reticulum complexes in neurons and astrocytes, J. Biol. Chem. 279 (2004) 2885–2893.
[41] M.P. Lisanti, P.E. Scherer, J. Vidugiriene, Z. Tang, A. Hermanowski-Vosatka, Y.H. Tu, R.F. Cook, M. Sargiacomo, Characterization of caveolin-rich membrane domains isolated from an endothelial-rich source: implications for human disease, J. Cell Biol. 126 (1994) 111–126.
[42] G. Radeva, F.J. Sharom, Isolation and characterization of lipid rafts with different properties from RBL-2H3 (rat basophilic leukaemia) cells, Biochem. J. 380 (2004) 219–230.
[43] J.L. Macdonald, L.J. Pike, A simplified method for the preparation of detergent-free lipid rafts, J. Lipid Res. 46 (2005) 1061–1067.
[44] J.H. Clark, N.P. Kinnear, S. Kalujnaia, G. Cramb, S. Fleischer, L.H. Jeyakumar, F. Wuytack, A.M. Evans, Identification of functionally segregated sarcoplasmic reticulum calcium stores in pulmonary arterial smooth muscle, J. Biol. Chem. 285 (2010) 13542–13549.

[45] S. Giusti, M.E. Bogetti, A. Bonafina, d.P. Fiszer, An improved method to obtain a soluble nuclear fraction from embryonic brain tissue, Neurochem. Res. 34 (2009) 2022–2029.
[46] E.D. Moore, T. Voigt, Y.M. Kobayashi, G. Isenberg, F.S. Fay, M.F. Gallitelli, C. Franzini-Armstrong, Organization of Ca2+ release units in excitable smooth muscle of the guinea-pig urinary bladder, Biophys. J. 87 (2004) 1836–1847.
[47] D. Poburko, C.H. Liao, V.S. Lemos, E. Lin, Y. Maruyama, W.C. Cole, C. van Breemen, Transient receptor potential channel 6-mediated, localized cytosolic [Na+] transients drive Na+/Ca2+ exchanger-mediated Ca2+ entry in purinergically stimulated aorta smooth muscle cells, Circ. Res. 101 (2007) 1030–1038.
[48] N. Calloway, M. Vig, J.P. Kinet, D. Holowka, B. Baird, Molecular clustering of STIM1 with Orai1/CRACM1 at the plasma membrane depends dynamically on depletion of Ca2+ stores and on electrostatic interactions, Mol. Biol. Cell 20 (2009) 389–399.
[49] T. Hewavitharana, X. Deng, J. Soboloff, D.L. Gill, Role of STIM and Orai proteins in the store-operated calcium signaling pathway, Cell Calcium 42 (2007) 173–182.
[50] A.C. Martin, D. Willoughby, A. Ciruela, L.J. Ayling, M. Pagano, S. Wachten, A. Tengholm, D.M. Cooper, Capacitative Ca2+ entry via Orai1 and stromal interacting molecule 1 (STIM1) regulates adenylyl cyclase type 8, Mol. Pharmacol. 75 (2009) 830–842.
[51] D.T. Browman, M.E. Resek, L.D. Zajchowski, S.M. Robbins, Erlin-1 and erlin-2 are novel members of the prohibitin family of proteins that define lipid-raft-like domains of the ER, J. Cell Sci. 119 (2006) 3149–3160.
[52] A.K. Grover, S.E. Samson, Pig coronary artery smooth muscle: substrate and pH dependence of the two calcium pumps, Am. J. Physiol. 251 (1986) C529–C534.
[53] A.K. Grover, C.Y. Kwan, S.E. Samson, Effects of peroxynitrite on sarco/endoplasmic reticulum Ca2+ pump isoforms SERCA2b and SERCA3a, Am. J. Physiol. Cell Physiol. 285 (2003) C1537–C1543.
[54] J. Bossuyt, B.E. Taylor, M. James-Kracke, C.C. Hale, Evidence for cardiac sodium–calcium exchanger association with caveolin-3, FEBS Lett. 511 (2002) 113–117.
[55] A. Cavalli, M. Eghbali, T.Y. Minosyan, E. Stefani, K.D. Philipson, Localization of sarcolemmal proteins to lipid rafts in the myocardium, Cell Calcium 42 (2007) 313–322.
[56] D.R. Scriven, A. Klimek, P. Asghari, K. Bellve, E.D. Moore, Caveolin-3 is adjacent to a group of extradyadic ryanodine receptors, Biophys. J. 89 (2005) 1893–1901.
[57] P.E. Bickel, P.E. Scherer, J.E. Schnitzer, P. Oh, M.P. Lisanti, H.F. Lodish, Flotillin and epidermal surface antigen define a new family of caveolae-associated integral membrane proteins, J. Biol. Chem. 272 (1997) 13793–13802.
[58] C. Bracho, I. Dunia, M. Romano, G. Raposo, R.M. De La, E.L. Benedetti, H.A. Perez, Caveolins and flotillin-2 are present in the blood stages of *Plasmodium vivax*, Parasitol. Res. 99 (2006) 153–159.
[59] V.O. Rybin, P.W. Grabham, H. Elouardighi, S.F. Steinberg, Caveolae-associated proteins in cardiomyocytes: caveolin-2 expression and interactions with caveolin-3, Am. J. Physiol. Heart Circ. Physiol. 285 (2003) H325–H332.
[60] S. Mishra, P.G. Joshi, Lipid raft heterogeneity: an enigma, J. Neurochem. 103 (Suppl 1) (2007) 135–142.
[61] A. Pralle, P. Keller, E.L. Florin, K. Simons, J.K. Horber, Sphingolipid–cholesterol rafts diffuse as small entities in the plasma membrane of mammalian cells, J. Cell Biol. 148 (2000) 997–1008.
[62] G.J. Schutz, G. Kada, V.P. Pastushenko, H. Schindler, Properties of lipid microdomains in a muscle cell membrane visualized by single molecule microscopy, EMBO J. 19 (2000) 892–901.
[63] S.H. Cha, S.Y. Shin, S.Y. Jung, Y.T. Kim, Y.J. Park, J.O. Kwak, H.W. Kim, C.K. Suh, Evidence for Na+/Ca2+ exchanger 1 association with caveolin-1 and -2 in C6 glioma cells, IUBMB Life 56 (2004) 621–627.